DYNAMIC ANALYSIS OF FIXED-FIXED BEAMS

A THESIS SUBMITTED IN PARTIAL FULFILMENT OF

THE REQUIREMENT FOR THE DEGREE OF

Master of Technology

in

Mechanical Engineering

(Specialisation: Machine Design and analysis)

By

HEMANTA KUMAR RANA

Roll No. 210ME1194

Department of Mechanical Engineering

National Institute of Technology

Rourkela-769008

May 2012

Dynamic Analysis of Fixed-Fixed Beams

A THESIS SUBMITTED IN PARTIAL FULFILMENT OF

THE REQUIREMENT FOR THE DEGREE OF

Master of Technology

in

Mechanical Engineering

(Specialisation: Machine Design and analysis)

By

HEMANTA KUMAR RANA

Roll No. 210ME1194

Under the guidance of

Prof. Bijoy Kumar Nanda

Department of Mechanical Engineering

National Institute of Technology, Rourkela

Department of Mechanical Engineering

National Institute of Technology

Rourkela-769008

May 2012

National institute of technology

Rourkela

CERTIFICATE

This is to certify that the work in the thesis entitled **"DYNAMIC ANALYSIS OF FIXED-FIXED BEAMS"** submitted by **Hemanta Kumar Rana** bearing Roll No. **210ME1194** in partial fulfillment of the requirements for the award of Master of Technology Degree in Mechanical engineering (Machine Design and Analysis) at National Institute of Technology, Rourkela is an authentic work carried out by him under my supervision and guidance. Neither this thesis nor any part of it has been submitted for any degree or academic award elsewhere.

Date:

Place: Rourkela

Prof. Bijoy Kumar Nanda

Department of Mechanical Engineering

National Institute of Technology

Rourkela – 769008

ACKNOWLEDGEMENTS

While bringing out this thesis to its final form, I came across a number of people whose contributions in various ways helped my field of research and they deserve special thanks. It is a pleasure to convey my gratitude to all of them.

First and foremost, I would like to express my deep sense of gratitude and indebtedness to my supervisor **Prof. B. K. Nanda** for his invaluable encouragement, suggestions and support from an early stage of this research and providing me extraordinary experiences throughout the work. Above all, his priceless and meticulous supervision at each and every phase of work inspired me in innumerable ways.

I specially acknowledge him for his advice, supervision, and the vital contribution as and when required during this research. His involvement with originality has triggered and nourished my intellectual maturity that will help me for a long time to come. I am proud to record that I had the opportunity to work with an exceptionally experienced Professor like him.

I am highly grateful to **Prof. S. K. Sarangi**, Director, National Institute of Technology, Rourkela, **Prof. R.K. Sahoo**, Former Head, Department of Mechanical Engineering and **Prof. K.P. Maity,** Head, Department of Mechanical Engineering for their kind support and permission to use the facilities available in the Institute.

I am obliged to **Asst. Prof. Bhagat Singh, Mrs. Arundhanti Pradhan, Mr.Shiba Narayan Sahu,** for their support and co-operation that is difficult to express in words. The time spent with them will remain in my memory for years to come.

Finally, I am deeply indebted to my mother, **Mrs. Ratnabati Rana**, my father, **Mr. Romanchal Rana,** my two loving younger sisters, **Mita** and **Reeta** and to my friends for their moral support and continuous encouragement while carrying out this study. I dedicate this thesis to almighty deity **Maa Manikeswari**.

Hemanta Kumar Rana

Abstract

Welded joints are often used to fabricate assembled structures in machine tools, automotive and many such industries requiring high damping and light weight. Many structures are made by connecting structural members through joints. Due to very low material damping of built-up structures, sufficient damping has to come from the joints. Damping in built-up structures is often caused by energy dissipation due to micro-slip along frictional interfaces which provides a beneficial damping mechanism and plays an important role in the vibration behaviour of such structures. The damping characteristics in jointed structures are influenced by the intensity of pressure distribution, micro-slip and kinematic coefficient of friction at the interfaces and the effects of all these parameters on the mechanism of damping have been extensively studied. The ultimate goal of this project is to develop a damping model that is capable of describing the effects of welded joints on a vibrating structure. To estimate the damping capacity of a welded and layered fixed-fixed beam; it is investigated through analytically and experimentally. The theoretical analysis proposes two different methods to evaluate damping: classical and finite element method. In view of any discrepancy in results, experiments are conducted for different sets of mild steel specimens under different vibrating conditions. Time domain approach has been adopted to evaluate experimentally the damping capacity of the fixed-fixed beams. Both the numerical and experimental results are compared for authentication. Finally, useful conclusions have been drawn from both the numerical and experimental results.

CONTENTS

LIST OF FIGURES

LIST OF TABLES

NOMENCLATURE

English Symbols

A	Area of cross-section of the beam
$\boldsymbol{d}^{e}$	Nodal displacement vector of an element
b	Width of the beam
$\mathbf{C}$	Damping matrix
$\mathbf{q}^{e}$	Nodal displacement vector
X	Global displacement vector
$\ddot{\mathrm{X}}$	Global acceleration vector
E	Static bending modulus of elasticity
E_{loss}	Total energy loss per cycle
E_{ne}	Maximum strain energy stored in the system
$T(t)$	Forcing time dependent displacement function
$2h$	Overall thickness of the beam of the welded beam
I	Moment of inertia of the cross-section of the beam
K_s	Static bending stiffness of the layered and jointed beam
$\mathbf{k}^{e}$	Element stiffness matrix
$\mathbf{K}$	Global stiffness matrix
l	Length of the layered and welded beam individual
m	Number of layers in a jointed beam
$\mathbf{m}^{e}$	Element mass matrix
$\mathbf{M}$	Global mass matrix
n	Number of finite elements

p Interface pressure

u_1 Displacement in the x-direction of points on the upper beam

u_2 Displacement in the x-direction of points on the lower beam

v_1 Vertical deflection of upper laminate

v_2 Vertical deflection of lower laminate

N_1, N_2, $N_,$ N' Cubic shape functions

t Time coordinate

u_r Relative dynamic slip at the interfaces

x_0, x_n Amplitude of first cycle and last cycle, respectively

$y\left(\frac{L}{2},0\right)$ Mid-span displacement

n Number of cycles

Greek Symbols

α Dynamic slip ratio

δ Logarithmic decrement of the system

Δ Deflection due to static load

μ Kinematic coefficient of friction

ω_n Natural frequency of vibration

ϕ Eigenvector or modal displacement

ρ Mass density

θ_1, θ_2 Slope at the nodes of an element

ξ Damping ratio

Superscripts

e Element

Operators

‘,’	$\frac{d}{dx}$
T	Transpose of a matrix

CHAPTER 1

INTRODUCTION

Problems involving vibration occur in many areas of mechanical, civil and aerospace engineering. Engineering structures are generally fabricated using a variety of connections such as bolted, riveted, welded and bonded joints etc. The dynamics of mechanical joints is a topic of special interest due to their strong influence in the performance of the structure. Further, the inclusion of these joints plays a significant role in the overall system behaviour, particularly the damping level of the structures. However, the determination of damping either by analysis or experiment is never straightforward owing to the complexity of the dynamic interaction of components. The estimation of damping in beam-like structures with passive damping approach is the essential problem addressed by the present research.

Friction damping takes place whenever two surfaces experience relative motion in the presence of friction. In case of a jointed structure, the relative motion between contacting layers is a function of normal load which arises from the tightening of the joints holding the components. When the joint is very loose, the normal load is insignificant and the contact surface experiences pure slip. Since no work is required to be done against friction, no energy is dissipated. On the other hand, when the joint is very tight, high normal loads cause the whole contact interface to stick. This results in no energy dissipation again since no relative motion is allowed at the interfaces. For normal loads lying between these two extremities, energy is dissipated and the maximum value of energy dissipation occurs within this range. The contact pressure between the surfaces is generated by the clamping action of the joints and plays a vital role in the joint properties. Due to uneven pressure distribution, a local relative motion termed as micro-slip occurs at the interfaces of the connecting members.

Micro-slip is the normal mechanism by which mechanical joints dissipate energy and therefore, a better understanding of its phenomenon is required for the study of damping effects in the jointed structures occurs only at lower excitation levels. When the excitation level is increased, both micro- and macro-slips occur at the jointed interfaces. Usually, the macro-slip is avoided as it leads to structural damage of the joints. The contribution of the micro-slip on the overall system damping is significant in spite of its low magnitude and is generally promoted in structural joint designs.

The energy dissipated in most real structures is often very small, so that an undamped analysis is sometimes realistic. When the damping is significant, its effect must be included

in the analysis particularly when the dynamic study of a structure is required. The energy of the vibrating system is dissipated by various mechanisms and often more than one mechanism may be present at the same time. Although the knowledge on the friction joint is limited, efforts have been put in the present investigation to study the damping aspect of the friction joints in built-up structures.

1.1 Damping

Damping is the energy dissipation properties of a material or system under cyclic stress. When a structure is subjected to an excitation by an external force then it vibrates in certain amplitude of vibration, it reduces as the external force is removed. This is due to some résistance offered to the structural member that may be internal or external. This resistance is termed as damping.

The origin and mechanism of damping are complex and sometimes difficult to comprehend. The energy of the vibrating system is dissipated by various mechanisms and often more than one mechanism may be present simultaneously. For convenience, damping is divided into two major groups identified as:

1) Material Damping
2) Structural damping

1.1.1 Material Damping

Internal damping, also called solid or material damping, is related to the energy dissipation within the volume of material. This mechanism is usually associated with internal reconstructions of the micro and macro structure ranging from crystal lattice to molecular scale effects, thermo-elasticity, grain boundary viscosity, point-defect relaxation, etc. [1, 2]. Besides, there are two types of internal damping: hysteretic damping and visco-elastic damping.

When materials are critically stressed, energy is dissipated internally within the material itself. Experiments by several investigators indicate that for most structural systems, the energy dissipated per cycle is independent of the frequency and approximately proportional to the stiffness of the system and square of amplitude of vibration. Internal damping fitting to this classification is termed as hysteretic damping. The energy loss per cycle is expressed as $E=\pi*k*\lambda*A*2$, where k, λ and A is the stiffness of the system, dimensionless damping factor depending on the property of the material and amplitude of vibration, respectively. The

magnitude of this damping is very small as compared to other types of damping. When a body having material damping is subjected to vibration, the stress-strain diagram shows a hysteresis loop whose area denotes the energy lost per cycle due to damping. The stress (σ) and strain (ε) relations at a point in a vibrating body possess a hysteresis loop as shown in Fig. 1.1. The area of the hysteresis loop gives the energy dissipation per unit volume of the material per stress cycle [1, 3]. This is termed as specific damping capacity (Ψ) and given by the cyclic integral $\psi=\oint \sigma \, d\mathcal{E}$.

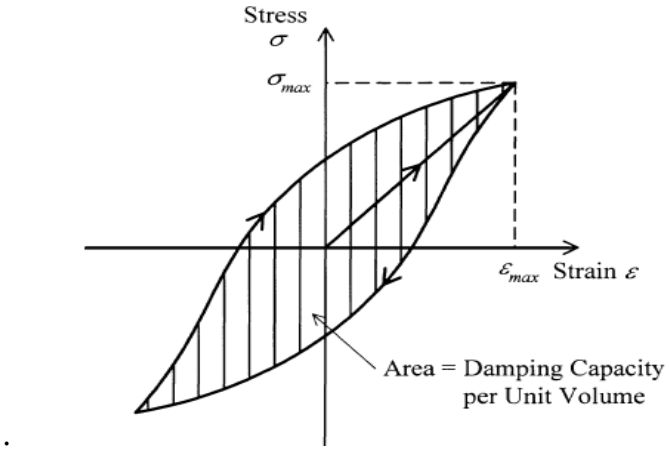

Fig. 1.1 a typical hysteresis loop for material damping

Passive damping using visco-elastic materials (VEM's) is widely used in both commercial and aerospace applications. Visco-elastics are elastomeric materials whose long-chain molecules cause them to convert mechanical energy into heat when they are deformed. The relation between the stress and strain of a visco-elastic damping material is expressed through a linear differential equation with respect to time.

The most widespread model used for visco-elastic damping is the Kelvin-Voigt model as it gives the most accurate results for practical purposes [1]. The stress-strain relationship given by this model is $\sigma= E\varepsilon+E^*\frac{d\varepsilon}{dt}$, where E and E* are the Young's modulus and complex modulus of the material, respectively. The term Eε represents the elastic behaviour of the material with no contribution to damping, while the second term $E^* \frac{d\varepsilon}{dt}$ is responsible for damping. The damping capacity per unit volume is expressed as

$$d_v=E^* \oint \frac{d\varepsilon}{dt} d\mathcal{E}$$

1.1.2 Structural Damping

Since the damping in the structural material is not significant, most of the damping in real fabricated structures arises in the joints and interfaces [1]. It is the result of energy dissipation caused by rubbing friction resulting from relative motion between components and by intermittent contact at the joints in a mechanical system. However, the energy dissipation mechanism in a joint is a complex phenomenon being largely influenced by the interface pressure and degree of slip at the interfaces. It is this slip phenomenon occurring in the presence of friction at the joint interface that causes the energy dissipation and nonlinearity in the joints.

1.2 Measurement of Structural Damping

There are several ways of expressing the damping in a structure. They are time response and frequency-response methods where the response of the system is expressed in terms of time and frequency, respectively. Depending on the mathematical model of the physical problem, the above two methods are used to measure the damping capacity of the structures. Logarithmic decrement (δ) is determined using time domain method and the quality factor (Q) by frequency domain method. However, the other nomenclatures such as; damping ratio (ζ), specific damping capacity (ψ) and loss factor (η) are estimated from either of the above two methods for measuring the damping.

1.2.1 Logarithmic Decrement (δ)

The logarithmic decrement method is the most widely used time-response method to measure damping from the free-decay of the time history curve.

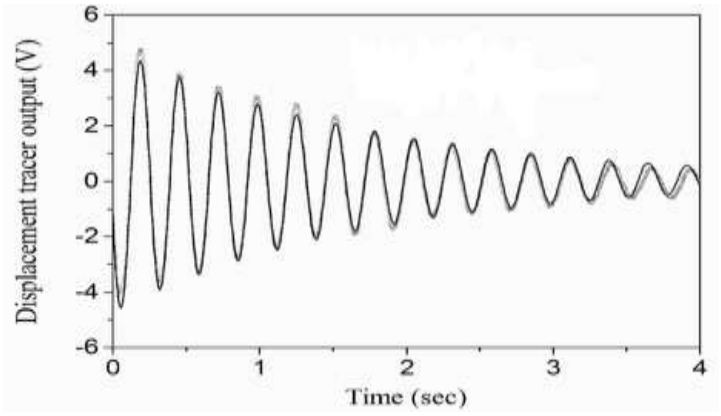

Fig. 1.2 Logarithmic Decrement

When the structure is set into free vibration, the fundamental mode dominates the response since all the higher modes are damped out quickly. The logarithmic decrement represents the rate at which the amplitude of a free damped vibration decreases. It is defined as the natural logarithm of the ratio of any two successive amplitudes. Thus, the logarithmic decrement δ is obtained as;

$$\delta = \ln\frac{x_1}{x_2} = \frac{2\pi\xi}{\sqrt{1-\xi^2}}$$

Where x_1 and x_2 are the successive amplitudes and ξis the damping ratio.

For small damping, the above relation is approximated as; $\delta \simeq 2\pi\xi$.

Generally for low damping, it is preferable to measure the amplitudes of oscillations of many cycles so that an accurately measurable difference exists. In such a case,

$$\delta = \frac{1}{n}\ln\left(\frac{x_0}{x_n}\right)$$

Where x_0 , x_n and n are the amplitudes of first and last cycles and number of cycles, respectively.

1.2.2 Damping Ratio (ζ)

It is defined as the ratio of the damping constant to the critical damping constant. The rate at which the motion decays in free vibration is controlled by the damping ratio ζ, which is a dimensionless measure of damping expressed as a percentage of critical damping. Figure 1.3 displays the free vibration response of several systems with varying levels of damping ratios. It is observed that the amplitude of vibration decays more rapidly as the value of the damping ratio increases.

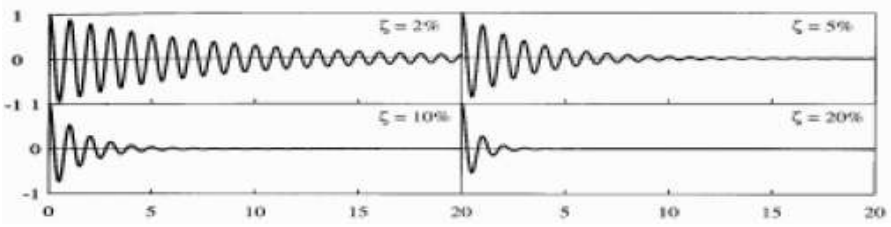

Fig. 1.3 Free vibration of systems with different levels of damping [2]

1.2.3 Specific Damping Capacity (Ψ)

The damping capacity is defined as the energy dissipated per complete cycle of vibration. The energy dissipation per cycle is calculated from the damping force (f_d) and is expressed in the integral form as;

$$\Delta U = \oint f_d \, dx$$

This is given by the area of the hysteresis loop in the displacement force-plane. The specific damping capacity (Ψ) is defined as the ratio of energy dissipated per cycle of vibration to the total energy of the system. If the initial (total) energy of the system is denoted by U_{max} , the specific damping capacity is given by;

$$\Psi = \frac{\Delta U}{U_{max}}$$

1.3 Linear Problem

Most structural problems are studied based on the assumption that the structure to be 6nalysed is either linear or nonlinear. In linear systems, the excitation and response are linearly related and their relationship is given by a linear plot as shown in Fig. 1.4. For many cases, this assumption is more often valid over certain operating ranges. Working with linear models is easier from both an analytical and experimental point of view. For beams undergoing small displacements, linear beam theory is used to calculate the natural frequencies, mode shapes and the response for a given excitation.

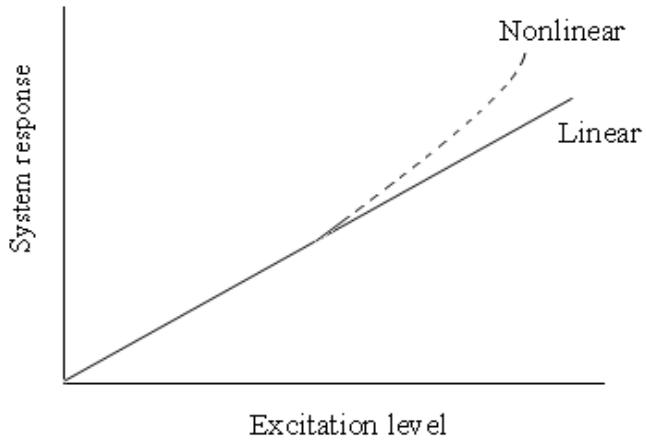

Fig. 1.4 Comparison of Linear and nonlinear systems

It is very clear from Fig. 1.3 that the linear and nonlinear systems agree well at small values of excitation, while they deviate at higher levels. The nonlinear beam theory is used for larger displacements where the superposition principle is not valid. The linear vibration theory is used when the beam is vibrated at small amplitudes and lower modes of vibration. The present investigation mainly focuses on the study of damping of jointed fixed-fixed beams at lower excitation levels which can be well considered as linear.

1.4 Beam Theories

The beam is one of the fundamental elements of an engineering structure and finds application in structural members like helicopter rotor blades, spacecraft antennae, flexible satellites, airplane wings, gun barrels, robot arms, high-rise buildings, long span bridges, etc. These beam-like structures are typically subjected to dynamic loads. Therefore, studying the static and dynamic response, both theoretically and experimentally, of these structural components under various loading conditions would help in understanding and explaining the behaviour of more complex and real structures.

The popular beam theories in use today are: (a) Euler-Bernoulli beam theory and (b) Timoshenko beam theory. Dynamic analysis of beams is generally based on one of the above beam theories. If the lateral dimensions of the beam are less than one-tenth of its length, then the effects of shear deformation and rotary inertia are neglected for the beams vibrating at low frequency. The no-transverse-shear assumption means that the rotation of cross section is due to bending alone. A beam based on such conditions is called Euler-Bernoulli beam or thin beam.

If the cross-sectional dimensions are not small compared to the length of the beam, the effects of shear deformation and rotary inertia are to be considered in the analysis. Timoshenko included these effects and obtained results in accordance with the exact theory. The procedure presented by Timoshenko is known as thick beam theory or Timoshenko beam theory. The present investigation is based on the assumptions of Euler-Bernoulli beam theory as the beam is vibrated at low frequency and the dimensions of test specimens are much smaller in the lateral directions compared to length, thus satisfying the condition of thin beam theory.

1.5 Modeling of a Structure

It is essential to have a theoretical model to represent a structure in order to study its dynamic characteristics. Theoretical 8nalysed8 of the present problem considers two approaches using the Euler-Bernoulli beam theory: classical model approach and finite element model approach.

A classical model is characterized by a partial differential equation with respect to spatial and time coordinates which is often used for studying simple structures such as a uniform beam. Exact solutions of such equations are possible only for a limited number of problems with simple geometry, boundary conditions and material properties.

However, real-life engineering structures are generally very complex in geometry, boundary conditions and material properties. For this reason, normally some kind of other approximate method is needed to solve a general problem.

The classical logarithmic decrement method is very popular for measuring damping in the time domain. This method is mostly used for free vibration response of a lightly damped linear system having low and medium frequency range. In this method, the damping is measured for a single frequency oscillation directly from the decay of the system response. It is established that this method is equally applicable to single as well as multiple degrees of freedom systems. In case of multiple degrees of freedom systems, the damping for each mode is separately determined if the decay of initial excitation takes place primarily in one mode of vibration.

1.6 Aims and Objectives:

As evident from the preceding discussions, built-up structures are generally assembled by bolted or riveted connections representing a significant source of damping. The dynamics of bolted structures have been studied by many investigators as evidenced from the wealth of published literatures. However, a little amount of research has been reported till date on the welded joints. Welding joints are widely used in aircraft, building constructions, trusses, frames, bridges and various other applications requiring high joint strength and damping. The use of welding in such applications is cheaper compared to other fasteners thereby giving low assembly cost. Further, welding is not susceptible to unintended loosening which might otherwise cause joint failures and hazardous environments. Moreover, the basic mechanism of energy loss due to interface friction and slip is same in case of all the fasteners. Therefore, an attempt has been made in the present investigation to study the mechanism of interface slip damping considering the above concept for layered and jointed welded structures.

CHAPTER 2

LITERATURE SURVEY

An important feature of built-up structures is the existence of slip at the interfaces of the structural components. The energy in such structures is dissipated through slipping, thereby emphasizing the need to study the mechanism of slip at the interfaces. In case of mechanical joints, the dissipation of energy takes place due to both micro and macro-slip [1]. On application of the force, small regions of the interface breaks encouraging slipping. These localized motions are termed as micro slip during which no relative motion takes place between the contacting surfaces. The micro-slip between the connecting members occurs only at lower excitation levels. With the application of more and more force on the joint, the entire contact area slips giving rise to macro-slip. Macro-slip usually leads to the failure of the joint and is generally avoided in all structural applications. However, the micro-slip provides a good level of energy dissipation without damaging the joint and is therefore encouraged in its design. Over the past few decades, most of the work has been confined in the area of micro and macro-slip phenomena [2, 3]. These concepts are utilized to study the dynamic behaviour of jointed structures having friction contact. The interface undergoes partial slip at high normal load. Masuko et al. [4] and Nishiwaki et al. [5, 6] have found out the energy loss in jointed cantilever beams considering micro-slip and normal force at the interfaces. Olofsson and Hagman [7] have shown that the micro-slip at the contacting surfaces occur when an optimum frictional load is applied. They have also presented a model for micro-slip between the flat smooth and rough surfaces covered with ellipsoidal elastic bodies.

The role of friction is of great significance in controlling the dynamic characteristics of engineering structures. The friction at the jointed interfaces arises when the layers have a relative movement under transverse vibration. The Coulomb's law of friction is widely used to represent the dry friction at the contacting surfaces. The friction in a joint arises from shearing between the parts and is governed by the tension in the bolt or rivet, surface properties and type of materials in contact [8]. Den Hartog [9] has analytically solved the steady state response of a simple friction-damped system with combined Coulomb and viscous friction.

The nature of pressure distribution across a beam layer is another important aspect affecting the damping capacity of jointed structures. Almost all previous researchers have

idealized the joints by assuming a uniform pressure profile without considering the effects of surface irregularities and asperities [4-6, 10,11]. In particular, Gould and Mikic [12] and Ziada and Abd [13] have reported that the pressure distribution at the interfaces of a bolted joint is parabolic in nature circumscribing the bolt which is approximately 3.5 times the bolt diameter.

Nanda and Behera [14] have developed a theoretical expression for the pressure distribution at the interfaces of a bolted joint by curve fitting the earlier data reported by Ziada and Abd [13]. They have obtained an eighth order polynomial even function in terms of normalized radial distance from the centre of the bolt such that the function assumes its maximum value at the centre of the bolt and decreases radially away from the bolt. They have used Dunn's curve fitting software to calculate the exact spacing between bolts that would result in a uniform interfacial pressure distribution along the entire length of the beam. Using exact spacing of 2.00211 times the diameter of the connecting bolts, Nanda and Behera have successfully simulated uniform interface pressure over the length of the beam. Thereafter, they have investigated the effect of interface pressure on the behaviour of interfacial slip damping.

There are various measuring methods available in practice to know the contact pressure between layers. However, the angle probe used by Minakuchi et al. [15] is more convenient to measure. They have found out the contact pressure between two layered beams of different thicknesses by establishing a relationship between the mean contact pressure and sound pressure of reflected waves. This method is widely accepted as the experimental results fairly agree with the theoretical ones.

Energy dissipation resulting from slip and non-uniform pressure distribution in bolted joints has been the subject of many studies [4-6,16]. Typically, the normal interfacial pressure across the clamped joint is not uniformly distributed. Under high pressure, the slip is small, while under low pressure the shear due to friction is small. An optimal clamping force exists somewhere between these two limits under which a joint dissipates maximum vibration energy. Beards [17] has looked into this aspect and recognized the existence of an optimum joint force for maximum energy dissipation.

It is very difficult to assess the joint properties correctly from the theoretical results and therefore, experiments are performed to verify the same. Nishiwaki et al. [5] have developed an improved band-width method to measure experimentally the damping capacity in terms of

logarithmic decrement of a bolted cantilever beam at first, second and third modes of vibration. Masuko et al. [4] and Nishiwaki et al. [6] have theoretically calculated the logarithmic decrement of a jointed cantilever beam considering the normal force and micro-slip at the interfaces. Recently, Olunloyo et al. [18] have analytically investigated the slip damping of layered visco-elastic beam plate structures using the logarithmic decrement approach. Damisa et al. [19] have performed a dynamic analysis of slip damping in clamped layered beams with non-uniform pressure distribution at the interfaces. They have shown that under dynamic loads, the frequency variation and non-uniformity in pressure distribution can have significant effect on both the energy dissipation and logarithmic damping decrement.

The finite element method is one of the numerical techniques for solving many boundary and initial value engineering problems. However, its application in damping analysis is relatively recent. Gaul and Lenz [20] have worked in detail on the finite element models considering slip mechanisms to study the dynamic response of assembled structures. Sainsbury and Zhang [21] have used the finite element procedure through Galerkin element method (GEM) to make the dynamic analysis of damped sandwich beam structures. Lee et al. [22] have used the finite element model of a jointed beam to obtain the natural frequencies and mode shapes. Chen and Deng [23] have carefully studied the micro-slip phenomenon using the finite element method under plane stress conditions. They have carried out investigations on two classical joint configurations for 12nalysed12: the press-fit joint and lap-shear joint. They have focused their work to evaluate the effect of dry friction and slip on the damping response of joints for quantifying the energy dissipation during cyclic loading. Oldfield et al. [24] have 12nalysed the effect of dynamic friction on energy dissipation of a bolted joint under harmonic loading by finite element method using Jenkins elements. They have studied the effect of preload on the interface pressure affecting the response of the joint. At high preload, little sliding occurs at the joint interface producing less frictional energy.

CHAPTER 3

THEORITICAL ANALYSIS BY CLASSICAL ENERGY APPROACH

This chapter gives a detailed description of the theoretical analysis by classical energy approach for determining the damping capacity in layered and jointed fixed-fixed beam with welded joints. A fixed-fixed beam model representing a continuous system based on the Euler-Bernoulli beam theory has been used for deriving the necessary formulation.

3.1 General Assumptions

Certain assumptions are made in the present analysis while treating joint dynamics. These include:

1) Each layer of the beam undergoes the same transverse deflection.
2) The local mass of the joint area is not considered as significant in altering the behaviour of the beam.
3) There is no displacement and rotation of the beam at the clamped end.
4) The material behaves linearly.
5) The deflections are small compared to the beam thickness.

3.2 Dynamic equation free transverse vibration

The beam vibration is governed by partial differential equations in terms of spatial variables x and time variable t. Thus, the governing differential equation for free vibration is given by:

$$EI\frac{d^4y}{dx^4}+\rho A\frac{d^2y}{dt^2}=0 \tag{3.1}$$

Where E, I, ρ andA are modulus of elasticity, second moment of area of the beam, mass density and cross-sectional area of the beam respectively. The free vibration given by eq. (3.1) contains four spatial derivatives and hence requires four boundary conditions for getting a solution. The presence of two time derivatives again requires two initial conditions, one for displacement and another for velocity.

Eq. (3.1) is solved by method of separation of variables. The displacement y(x, t) is written as the product of two functions, one depends on only x and other depends only on t. Thus the solution is expressed as:

$$y(x,t) = X(x) \times T(t) \tag{3.2}$$

Where X(x) and T (t) are the space and time function respectively.

Substituting eq. (3.2) into eq. (3.1) and rearrange results;

$$EIT(t)\frac{d^4X}{dx^4} = -\rho AX\left(x\right)\frac{d^2T}{dt^2} \tag{3.3}$$

Dividing eq. (3.3) by X (x)*T (t) on both sides, variables are separated as;

$$\frac{\frac{d^2T}{dt^2}}{T(t)} = -\frac{EI}{\rho A}\frac{\frac{d^4X}{dx^4}}{X(x)} = \omega_n^2 \tag{3.4}$$

Where the term ω_n^2 is the separation constant, representing the square of natural frequency.

This equation yields two ordinary differential equations.

The first one is given as;

$$\frac{d^4X}{dx^4} - \lambda^4 X(x) = 0 \tag{3.5}$$

Where $\lambda^4 = \frac{\rho A}{EI}\omega_n^2$

The required solution of eq. (3.5) is simplified as;

$$X(x) = A_1 \sin\lambda x + A_2 \cos\lambda x + A_3 \sinh\lambda x + A_4 \cosh\lambda x \tag{3.6}$$

Where constant $A_1, A_2, A_3 and A_4$ are determined from the boundary conditions of fixed-fixed beam.

The second equation is given as;

$$\frac{d^2T}{dt^2} + \omega_n^2 T(t) = 0 \tag{3.7}$$

This is the similar free vibration expression for an un-damped single degree of freedom system having the solution

$$T(t) = A_5 \cos \omega_n t + A_6 \sin \omega_n t \tag{3.8}$$

Substituting the expression for space and time function as given by eq. (3.6) and eq. (3.8) into eq. (3.2), the complete solution for the deflection of a beam at any section is expressed as;

$$y(x,t) = (A_1 \sin \lambda x + A_2 \cos \lambda x + A_3 \sinh \lambda x + A_4 \cosh \lambda x) \times (A_5 \cos \omega_n t + A_6 \sin \omega_n t) \tag{3.9}$$

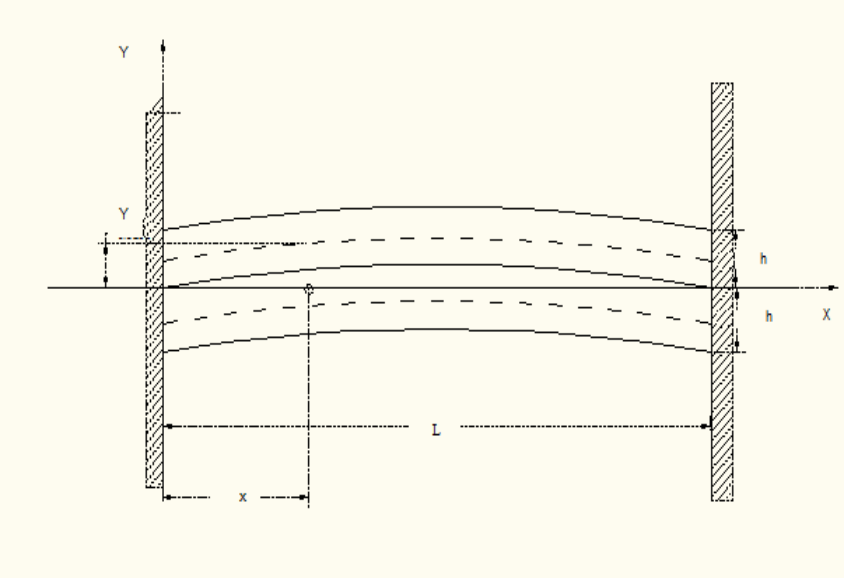

Fig. 3.1 Differential analysis of a beam

3.2.1 Evaluation of Constants $A_1, A_2, A_3 and A_4$

The boundary conditions for the fixed-fixed beam are given as;

At $x = 0$; $\quad X(0) = 0$; $\quad X'(0) = 0$;

At $x = L$; $\quad X(L) = 0$; $\quad X'(L) = 0$

Writing the expression of space function as given in eq. (3.6) and its first derivative are written as;

$$X(x) = A_1 \sin \lambda x + A_2 \cos \lambda x + A_3 \sinh \lambda x + A_4 \cosh \lambda x \tag{3.9a}$$

$$X'(x) = \lambda \left(A_1 \cos \lambda x - A_2 \sin \lambda x + A_3 \cosh \lambda x + A_4 \sinh \lambda x \right) = 0 \tag{3.9b}$$

Putting the boundary conditions, eq. (3.9) is reduced to

$$X(0) = A_2 + A_4 = 0; \tag{3.10a}$$

$$X'(0) = A_1 + A_3 = 0; \tag{3.10b}$$

$$X(L) = A_1 \sin \lambda L + A_2 \cos \lambda L + A_3 \sinh \lambda L + A_4 \cosh \lambda L = 0 \tag{3.10c}$$

$$X'(x) = \lambda \left(A_1 \cos \lambda L - A_2 \sin \lambda L + A_3 \cosh \lambda L + A_4 \sinh \lambda L \right) = 0$$

i.e., $A_1 \cos \lambda L - A_2 \sin \lambda L + A_3 \cosh \lambda L + A_4 \sinh \lambda L = 0$ (3.10d)

The eq. (3.10) can be represented in a matrix form as;

$$\begin{bmatrix} 0 & 1 & 0 & 1 \\ 1 & 0 & 1 & 0 \\ \sin \lambda L & \cos \lambda L & \sinh \lambda L & \cosh \lambda L \\ \cos \lambda L & -\sin \lambda L & \cosh \lambda L & \sinh \lambda L \end{bmatrix} \begin{Bmatrix} A_1 \\ A_2 \\ A_3 \\ A_4 \end{Bmatrix} = \begin{Bmatrix} 0 \\ 0 \\ 0 \\ 0 \end{Bmatrix} \tag{3.11}$$

To get a non-trivial solution, setting the determinant equal to zero;

$$\begin{bmatrix} 0 & 1 & 0 & 1 \\ 1 & 0 & 1 & 0 \\ \sin \lambda L & \cos \lambda L & \sinh \lambda L & \cosh \lambda L \\ \cos \lambda L & -\sin \lambda L & \cosh \lambda L & \sinh \lambda L \end{bmatrix} = 0 \tag{3.12}$$

The characteristic equation is given as;

$$\cos(\lambda L)\times\cos(\lambda L)=1 \tag{3.12}$$

The constant $A_2, A_3 and A_4$ are dependent parameter but A_1 is an independent parameter. A_1 may have any values. Taking $A_1=1$, the values $A_2, A_3 and A_4$ of are found as;

$$A_2=\left(\frac{\sinh\lambda L-\sin\lambda L}{\cos\lambda L-\cosh\lambda L}\right);\ A_3=-1;\ A_4=-\left(\frac{\sinh\lambda L-\sin\lambda L}{\cos\lambda L-\cosh\lambda L}\right);\ A_1=1$$

Now space function given by eq. (3.6) is modified as;

$$X(x)=\sin\lambda x+\left(\frac{\sinh\lambda L-\sin\lambda L}{\cos\lambda L-\cosh\lambda L}\right)\cos\lambda x-\sinh\lambda x-\left(\frac{\sinh\lambda L-\sin\lambda L}{\cos\lambda L-\cosh\lambda L}\right)\cosh\lambda x$$

i.e., $$X(x)=\frac{(\sin\lambda x-\sinh\lambda x)(\cos\lambda L-\cosh\lambda L)+(\cos\lambda x-\cosh\lambda x)(\sinh\lambda L-\sin\lambda L)}{\cos\lambda L-\cosh\lambda L} \tag{3.13}$$

This equation gives the different mode shapes of vibration.

3.2.2 Evaluation of constants $A_5 and A_6$

The general expression of deflection at any section of beam is given in eq. (3.9) is written as;

$$Y(x,t)=X(x)\times(A_5\cos\omega_n t+A_6\sin\omega_n t) \tag{3.14}$$

Taking the derivative with respect to time, the above equation reduced to;

$$Y'(x,t)=X(x)\times(-A_5\omega_n\sin\omega_n t+A_6\omega_n\cos\omega_n t) \tag{3.15}$$

The velocity of deflection at the mid-span of the beam is zero.

i.e., $Y'\left(\frac{L}{2},0\right)=0$ this yields $A_6=0$;

Hence the eq. (3.14) reduced to;

$$Y(x,t)=X(x)\times(A_5\cos\omega_n t) \tag{3.16}$$

The deflection at the mid-span of the beam is taken equal to $X\left(\frac{L}{2}\right)$ and substituting the same in eq. (3.16), we obtained;

$$y\left(\frac{L}{2},0\right)=X\left(\frac{L}{2}\right)\times A_5$$

i.e. $$A_5=\left[\frac{y\left(\frac{L}{2},0\right)}{X\left(\frac{L}{2}\right)}\right]$$

Substituting the values of A_5 in eq. (3.16), the final equation for the deflection is found to be;

$$y(x,t)=X(x)\times\left[\frac{y\left(\frac{L}{2},0\right)}{X\left(\frac{L}{2}\right)}\right](\cos\omega_n t)$$

i.e.,

$$y(x,t)=\left[\begin{matrix}(\sin\lambda x-\sinh\lambda x)(\cos\lambda L-\cosh\lambda L)+\\(\cos\lambda x-\cosh\lambda x)(\sinh\lambda L-\sin\lambda L)\end{matrix}\right]\left[\frac{y\left(\frac{L}{2},0\right)}{X\left(\frac{L}{2}\right)}\right]\frac{\cos\omega_n t}{(\cos\lambda L-\cosh\lambda L)} \tag{3.17}$$

This is the generalized deflection equation at any section of a fixed-fixed beam.

3.3 Evaluation of relative dynamic slip:

The relative slip at the interface in the presence of friction during the vibration is given as;

$$u_r(x,t) = \alpha u(x,t) = 2\alpha h \tan\left[\frac{\partial y(x,t)}{\partial x}\right] \tag{3.18}$$

Where α = slip ratio

h = thickness of the beam

$y(x,t)$ = Deflection at a distance 'x' from the fixed end

$u(x,t)$ = Dynamic slip without friction

3.4 Analysis of energy dissipated:

The energy is dissipated due to the friction and relative dynamic slip at the interface is given by;

$$E_{loss} = 2\int_0^{\frac{\pi}{\omega_n}} \int_0^{\frac{L}{2}} \mu p b \left[\frac{\partial u_r(x,t)}{\partial t}\right] dx dt \tag{3.19}$$

Where μ = coefficient of kinematic friction

p = uniform pressure distribution at the interface

L= length of the beam

ω_n = natural frequency of vibration

The strain energy per half cycle of vibration is given by

$$E_{ne} = \left(\frac{192EI}{L^3}\right) y^2\left(\frac{L}{2},0\right) \tag{3.20}$$

Where E= modulus of elasticity

$I = \frac{b(2h)^3}{12}$, cross-sectional moment of inertia of the beam

$y\left(\frac{L}{2},0\right)$ = Transverse deflection at the mid-point of the fixed-fixed beam

Substituting eq. (3.18) into eq. (3.19) and is given by;

$$E_{loss} = 4\alpha h\mu pb\int_0^{\frac{\pi}{\omega_n}}\int_0^{\frac{L}{2}}\left\{\frac{\partial\left\{\tan\left(\partial y(x,t)/\partial x\right)\right\}}{\partial t}\right\}dxdt \tag{3.21}$$

The slop is very small i.e. $\tan\left(\frac{\partial y(x,t)}{\partial x}\right) = \frac{\partial y(x,t)}{\partial x}$;

Hence eq. (3.21) reduced to

$$E_{loss} = 4\alpha h\mu pb\int_0^{\frac{\pi}{\omega_n}}\int_0^{\frac{L}{2}}\left\{\partial^2 y(x,t)/\partial x\partial t\right\}dxdt \tag{3.22}$$

The ratio of dissipated energy and strain energy is found out dividing eq. (3.22) by eq. (3.20) is given by;

$$\frac{E_{loss}}{E_{ne}} = \frac{4\alpha h\mu pby\left(\frac{L}{2},0\right)}{\left(\frac{192EI}{L^3}\right)y^2\left(\frac{L}{2},0\right)}\int_0^{\frac{\pi}{\omega_n}}\int_0^{\frac{L}{2}}\left\{\partial^2 y(x,t)/\partial x\partial t\right\}dxdt \tag{3.23}$$

Substituting the boundary and initial conditions eq. (3.23) reduced to

$$\frac{E_{loss}}{E_{ne}} = \frac{8\alpha h\mu pby\left(\frac{L}{2},0\right)}{\left(\frac{192EI}{L^3}\right)y^2\left(\frac{L}{2},0\right)} \tag{3.23}$$

$$\frac{E_{loss}}{E_{ne}} = \frac{8\alpha h\mu pby\left(\frac{L}{2},0\right)}{K_s y^2\left(\frac{L}{2},0\right)} \tag{3.24}$$

Where K_s= static bending stiffness of fixed-fixed beam

3.5 Logarithmic decrement

Logarithmic decrement(δ), a measure of damping capacity, is defined as the natural logarithm of the ratio of two consecutive amplitudes in a given cycle.

$$\delta = \frac{1}{n}\ln\left(\frac{x_0}{x_n}\right) \tag{3.25}$$

Where x_0= amplitude of vibration of first cycle

x_n= amplitude of vibration of last cycle

n = number of cycles

Logarithmic decrement can also be written as;

$$\delta = \frac{1}{2}\left(\frac{E_{loss}}{E_{ne}}\right) \tag{3.26}$$

Where E_{loss} and E_{ne} are the energy loss due to interface friction and the total energy of the beam, respectively.

Substituting the eq. (3.24) into eq. (3.26) and given as;

$$\delta = \left[\frac{4\alpha h\mu pb}{K_s y\left(\frac{L}{2},0\right)}\right] \tag{3.27}$$

This is the generalized expression for numerical evaluation of logarithmic decrement for two layered fixed-fixed beams of any thickness.

3.6 Evaluation of damping ratio

The damping ratio, ξ , is expressed as the ratio of energy dissipated due to the relative dynamic slip at the interfaces and the total energy introduced into the system and is found to be;

$$\xi = \left[E_{loss}/\left(E_{loss}+E_{ne}\right)\right] = 1/\left[1+E_{ne}/E_{loss}\right] \tag{3.28}$$

Putting the values of E_{loss}/E_{ne} from expression (3.20) in (3.22) we get;

$$\xi = \frac{1}{1+\left[K_s y\left(\frac{L}{2},0\right)\right]\Big/\left[8\mu bph\alpha\right]} \tag{3.29}$$

Since, the above expression is valid for two-layered and jointed fixed-fixed beam; a generalized expression has been developed for a multi-layered and jointed cantilever beam as given by;

$$\xi = \frac{1}{1+\left[K_s y\left(\frac{L}{2},0\right)\right]\Big/\left[8(m-1)\mu bph\alpha\right]} \tag{3.30}$$

where, m is the number of layers.

It is very difficult to assess the damping produced in the joints due to variations of the above two vital parameters (α and μ) under dynamic conditions. These two parameters are inter-dependent and if one is increasing, the other is decreasing and vice versa. However, their product ($\alpha.\mu$) is found to be constant for a particular specimen. Thus, this product $\alpha.\mu$ is found out modifying expressions (3.26) and (3.28) as;

$$\alpha.\mu = K_s\left(1-e^{-2\delta}\right)y\left(\frac{L}{2},0\right)\Big/8bphe^{-2\delta} \tag{3.31}$$

This product has been found out from the experimental results of logarithmic decrement for a particular welded beam of 3 mm thickness using the expression (3.31) and subsequently used to find out the numerical values of the logarithmic decrement for other conditions of the beam using expressions (3.27) and (3.30).

CHAPTER 4

FINITE ELEMENT METHOD

Many practical problems in engineering deal with complicated shapes with arbitrary boundary conditions whose analysis becomes extremely difficult and in a few cases almost impossible by the conventional methods. Therefore, various numerical techniques have been developed to solve all these complicated engineering problems. One of such numerical techniques used is the finite element method in which an approximate solution is achieved by discretized the problem into many sub domains and this sub domain is called a finite element.

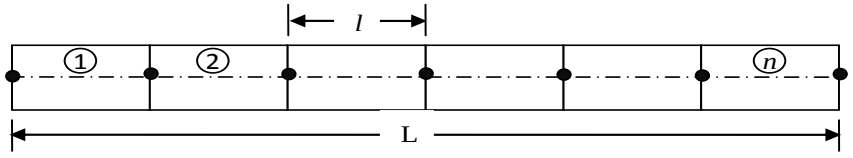

Fig. 4.1 Mess of n number of beam elements

There are two common types of numerical methods: (1) finite difference methods and (2) finite element methods. In the finite difference methods, the differential equation is written for each node and the derivatives are replaced by difference equations. This approach results in a set of simultaneous linear equations. Although finite difference methods are easy to adopt in simple problems, but their application becomes difficult to problems with complex geometries or boundary conditions.

Each element is free to deform and may have different material and geometrical properties. The proper choice of the element varies from one-dimensional axial element to three-dimensional solid element depending upon the nature of problem. The elements considered in the present investigation are one-dimensional beam elements representing the neutral axis of the beam. These elements are considered to be interconnected at specified joints called nodes. These nodes usually lie on the element boundaries where adjacent elements are considered to be connected.

The variation of the field variable within a finite element is approximated by a simple function called shape function. The shape function dictates the size of these nodal contributions. Further, the element stiffness and mass matrices of the individual elements are evaluated. The governing equations for each element are derived and assembled to find out

the system equations describing the behaviour of the body. Thus, each individual element and its contributions are considered adequately in obtaining a global model for a structure.

The damping matrix has been evaluated considering the Rayleigh damping matrix. These stiffness, mass and damping matrices are further used to evaluate the natural frequency and mode shapes of the layered and welded fixed-fixed beams.

4.1 The Displacement Description

At each node n, three displacements $\{q_n\}$ are introduced, these being the transverse displacement w_n, the rotation θ_n and the axial displacements u_{n1} at the joint of these elastic layers

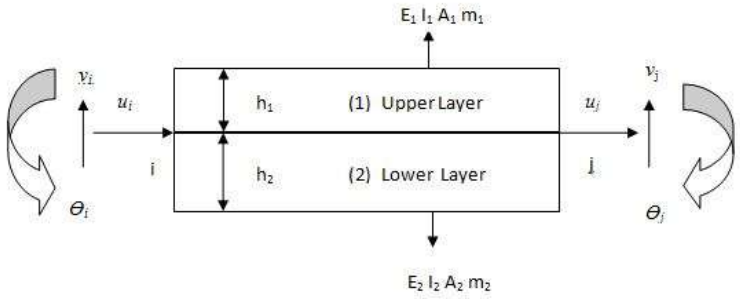

Fig.4.2 Finite element model for the damped layered and welded beams

The total set of nodal displacements for the element is given by:

$$\left\{q^e\right\} = \left\{u_1 \quad v_1 \quad \theta_1 \quad u_2 \quad v_2 \quad \theta_2\right\}^T \tag{4.1}$$

The displacement field vector {d} is expressed in terms of the polynomial shape functions as;

$$\begin{pmatrix} u_1 \\ v \\ \theta \end{pmatrix} = \begin{bmatrix} N_1 \\ N \\ N^{'} \end{bmatrix} \left\{q^e\right\} \tag{4.2}$$

$[N_1 \quad N \quad N^{\cdot}]$ Are the cubic shape functions given by;

$$\left[N_1\right] = \left\{1-\zeta \quad 0 \quad 0 \quad \zeta \quad 0 \quad 0\right\} \tag{4.3}$$

$$\left[N\right] = \left\{0 \quad 1-3\zeta^2+\zeta^3 \quad \left(\zeta-2\zeta^2+\zeta^3\right)l \quad 0 \quad 3\zeta^2-2\zeta^3 \quad \left(-\zeta^2+\zeta^3\right)l\right\} \tag{4.5}$$

$$\left[N'\right]=\left[\frac{\partial N}{\partial x}\right]=\frac{1}{l}\left[\frac{\partial N}{\partial \zeta}\right] \tag{4.6}$$

Where $\zeta = x/l$, l =element length.

4.1 Element Stiffness Matrix

The stiffness matrix for the jointed element is obtained from the bending strain energies as follows:

$$U_{be}=\frac{1}{2}\int_V \left(\varepsilon_1\sigma_1+\varepsilon_2\sigma_2\right)dV \tag{4.7}$$

$$U_{be}=\frac{1}{2}\int_0^l \left\{E_1I_1\left(\frac{\partial^2 w}{\partial x^2}\right)^2+E_1A_1\left(\frac{\partial u_1}{\partial x}\right)^2\right\}dx \tag{4.8}$$

$$U_{be}=\frac{1}{2}\left\{\mathbf{q^e}\right\}^T\int_0^1\left\{\frac{E_1I_1}{l^3}\left[N''\right]^T\left[N''\right]+\frac{E_1A_1}{l}\left[N_1'\right]^T\left[N_1'\right]\right\}d\xi\left\{\mathbf{q^e}\right\} \tag{4.9}$$

$$U_{be}=\frac{1}{2}\left\{\mathbf{q^e}\right\}^T\left[\mathbf{k}\right]^{\mathbf{e}}\left\{\mathbf{q^e}\right\} \tag{4.10}$$

Therefore, element stiffness matrix is given by;

$$\left[\mathbf{k}\right]^{\mathbf{e}}=\int_0^1\left\{\frac{E_1I_1}{l^3}\left[N''\right]^T\left[N''\right]+\frac{E_1A_1}{l}\left[N_1'\right]^T\left[N_1'\right]\right\}d\xi \text{ (4.11)} \tag{4.11}$$

Where E_i, A_i, I_i are the modulus of elasticity, cross-section area and moment of inertia of the ith layer of the beam. Integrating the expression (4.11), the element stiffness matrix is found to be;

$$\left[K^e\right]=\begin{bmatrix} \frac{EA}{l} & 0 & 0 & -\frac{EA}{l} & 0 & 0 \\ 0 & \frac{12EI}{l^3} & \frac{6EI}{l^2} & 0 & -\frac{12EI}{l^3} & \frac{6EI}{l^2} \\ 0 & \frac{6EI}{l^2} & \frac{4EI}{l} & 0 & -\frac{6EI}{l^2} & \frac{2EI}{l} \\ -\frac{EA}{l} & 0 & 0 & \frac{EA}{l} & 0 & 0 \\ 0 & -\frac{12EI}{l^3} & -\frac{6EI}{l^2} & 0 & \frac{12EI}{l^3} & -\frac{6EI}{l^2} \\ 0 & \frac{6EI}{l^2} & \frac{2EI}{l} & 0 & -\frac{6EI}{l^2} & \frac{4EI}{l} \end{bmatrix} \tag{4.12}$$

Where $EI = E_1 I_1 + E_2 I_2$, $AE = A_1 E_1 + A_2 E_2$

4.2 Element Mass Matrix

Following a similar procedure, the mass matrix for the jointed and welded beam element is obtained from the kinetic energy as follows:

$$T = \frac{1}{2}\int_0^l \left(m_0 \dot{w}^2 + m_1 \dot{u}_1^2\right) dx \tag{4.13}$$

Where m_i is the mass per unit length of the ith layer of the beam element and $m_0 = m_1 + m_2$

$$T = \frac{l}{2}\left\{\dot{\mathbf{q}}^{\mathbf{e}}\right\}^T \int_0^1 \left(m_0 \left[N\right]^T \left[N\right] + m_1 \left[N_1\right]^T \left[N_1\right]\right) d\xi \left\{\dot{\mathbf{q}}^{\mathbf{e}}\right\} \tag{4.14}$$

$$T = \frac{1}{2}\left\{\dot{\mathbf{q}}^{\mathbf{e}}\right\}^T \left[m\right]^e \left\{\dot{\mathbf{q}}^{\mathbf{e}}\right\} \tag{4.15}$$

Therefore, element mass matrix is given by;

$$\left[\mathbf{m}\right]^{\mathbf{e}} = \int_0^1 \left(m_1 \left[N\right]^T \left[N\right] + m_2 \left[N\right]^T \left[N\right]\right) d\xi \tag{4.16}$$

Integrating the expression (4.16), the element mass matrix is found to be;

$$\left[M^{e}\right]=\begin{bmatrix} \frac{m_0 l}{3} & 0 & 0 & \frac{m_0 l}{3} & 0 & 0 \\ 0 & \frac{13m_0 l}{35} & \frac{11m_0 l^2}{210} & 0 & \frac{9m_0 l}{70} & -\frac{13m_0 l^2}{420} \\ 0 & \frac{11m_0 l^2}{210} & \frac{11m_0 l^3}{105} & 0 & -\frac{13m_0 l^2}{140} & -\frac{m_0 l^3}{140} \\ \frac{m_0 l}{3} & 0 & 0 & \frac{m_0 l}{3} & 0 & 0 \\ 0 & \frac{9m_0 l}{70} & -\frac{13m_0 l^2}{420} & 0 & \frac{13m_0 l}{35} & \frac{11m_0 l^2}{210} \\ 0 & -\frac{13m_0 l^2}{140} & -\frac{m_0 l^3}{140} & 0 & \frac{11m_0 l^2}{210} & \frac{m_0 l^3}{105} \end{bmatrix} \tag{4.17}$$

Where $m_0 = m_1 + m_2$

4.3 Global Stiffness and Mass Matrix

The individual element stiffness and mass matrices are assembled to obtain the global stiffness and mass matrix for the jointed beam.

While adding the element-stiffness matrices, the elements of $\mathbf{k}^{\mathbf{e}}$ are placed in the appropriate locations of the global **K** matrix, based on the element connectivity; overlapping elements are simply added. This assembly is denoted symbolically as;

$$\sum_{\mathbf{e}} \mathbf{k}^{\mathbf{e}} \rightarrow \mathbf{K} \tag{4.18}$$

Similarly, the global mass matrix is assembled using the element mass matrices as given by;

$$\sum_{\mathbf{e}} \mathbf{m}^{\mathbf{e}} \rightarrow \mathbf{M} \tag{4.19}$$

4.4 Natural Frequencies and Mode Shapes

In all practical cases, the vibration always occurs at certain frequencies known as natural frequencies which follow the well-defined deformation patterns known as mode shapes. The study of natural frequencies and mode shapes in a vibrating system is known as modal analysis.

The modes are characterized by the eigenvalues and eigenvectors representing the natural frequencies and mode shapes, respectively. The global mass and stiffness matrices are utilized to determine the natural frequencies of vibration and mode shapes. The effect of

damping is generally neglected in the determination of natural frequencies and mode shapes of a lightly vibrating system. Therefore, real eigenvalues and eigenvectors are derived from the assumed undamped equation of motion. This assumption fairly holds well in most of the practical cases where damping is less pronounced.

4.5 Evaluation of Eigenvalues and Eigenvectors

The basic computational Eigen solution is determined in terms of mode shape by solving the expression as given by;

$$\mathbf{M}\ddot{\mathrm{X}} + \mathbf{K}\,\mathrm{X} = 0 \tag{4.20}$$

Where X and $\ddot{\mathrm{X}}$ are the displacement and acceleration vectors of all the nodes of the entire structure; **K** and **M** are the global stiffness and mass matrices, respectively.

4.6 Determination of Natural Frequencies

The natural frequency is an important parameter in the dynamic analysis of structures. If a system is excited by an external force and both the exciting and natural frequencies are very close to each other or equal, the resonant condition will occurs, thereby resulting violent vibration of the structure. This condition often leads to the catastrophic failure of the system. Therefore, it becomes necessary to design the dynamic system for its safe operation.

Generally, the micro-slip at the interfaces due to initial excitation of the jointed beam is more at lower modes than the higher ones as established by Nishiwaki et al. [6]. Moreover, Clough and Penzien [27] have shown that the mathematical idealization of any structural system is more reliable at lower modes of vibration. Considering all these, the higher modes are usually ignored in the dynamic analysis of structures. Therefore, the few modes of vibration have been taken into account in the present investigation neglecting the effect of higher modes.

The equation of motion for free vibration as given in expression (7.17) represents a generalized linear eigenvalue problem and its solution is given by;

$$X = \phi e^{i\omega t} \tag{4.21}$$

Where ϕ and ω are the mode shapes (eigenvector) and natural frequency (eigenvalue) of vibration, respectively.

Substituting expression (7.18) in (7.17) results;

$$\left[\mathbf{K}-\omega^2\mathbf{M}\right]\boldsymbol{\phi}=\boldsymbol{0} \tag{4.22}$$

In order to obtain a non-trivial solution, the determinant of coefficient matrix must be equal to zero, i.e.

$$\left|\mathbf{K}-\omega^2\mathbf{M}\right|=\boldsymbol{0} \tag{4.23}$$

An algebraic polynomial equation is obtained in ω^2 after expanding the above determinant. The roots of this equation give the eigenvalues representing natural frequencies of the system. The solution for ω produces pairs of positive and negative values of equal magnitude. The negative values of ω are usually ignored. The positive values of ω must be ordered so that the first lowest frequency is the fundamental frequency.

4.8 Damping Matrix

In the present analysis, Rayleigh damping is assumed. The element damping matrix is given by;

$$\left[\mathbf{C}\right]=\alpha\left[\mathbf{M}\right]+\beta\left[\mathbf{K}\right] \tag{4.25}$$

Where α and β are the Rayleigh damping coefficients and are determined from the experimental results. For the layered and welded beam, the first two computed natural frequencies are;

$\omega_1 = 207.3$ rad/s. $\omega_2 = 571.5$ rad/s.

The first two experimentally determined damping ratios are;

$\xi_1 = 0.00563$ $\xi_2 = 0.004987$

The Rayleigh damping coefficients are evaluated using the values of natural frequencies and damping ratios as follows;

$$\alpha=\frac{2\omega_1\omega_2\left(\xi_1\omega_2-\xi_2\omega_1\right)}{\omega_2^2-\omega_1^2}=1.8S^{-1}$$

$$\beta=\frac{2\left(\xi_2\omega_2-\xi_1\omega_1\right)}{\omega_2^2-\omega_1^2}=1.18\times10^{-5}S$$

CHAPTER 5

EXPERIMENTAL ANALYSIS

In the previous chapters, the classical and finite element methods for the evaluation of damping capacity in layered and welded fixed-fixed beams have been discussed in details. In real working conditions, the experimental study of damping becomes necessary as the theoretically computed results may vary from that of the actual values due to the various assumptions made in the theoretical analysis. Damping is purely a dynamic characteristic of a system which needs to be measured by conducting the dynamic tests on a structure. A number of experiments have been conducted using mild steel beam specimens in order to find out the damping capacity in terms of logarithmic decrement.

5.1 Specimen Details

The test specimens of different sizes are prepared from the stock of commercial mild steel. The two layered specimens are prepared by tack welding at the sides of the specimens. The distance between the tacks has been varied in steps. Further, specimens of various thicknesses and length are also prepared for conduct the experiments.

Sufficient care has been taken while welding in order to ensure the following salient features by the tack welded joints;

- Holds the assembled components in place and establishes their mutual location
- Ensures their alignment
- Controls movement and distortion during welding
- Sets and maintains the joint gap
- Ensures the assembly's mechanical strength against the external loading

The sequence and the direction of the tack welds are important for distortion control. Besides maintaining the joint gap, tack welds must resist transverse shrinkage to ensure sufficient rigidity. Tack welding should start at the middle and proceed along the joint length, alternating in both directions with proper back step or skip sequence for avoiding stress build-up and deformation. Tack welding can also be carried out by welding at the ends along the length first. Then, the tack welds are placed at the middle of each resulting distance between the previous welds. This procedure is repeated until the whole length at the appropriate locations is covered with the required number of welds.

5.2 Preparation of tack welded mild steel specimens

The specimens are prepared from the stock of mild steel flats by tack welding two layers of various thicknesses as presented in Tables 5.1. The mild steel flats are welded using the shielded metal arc welding technique. Shielded metal arc welding is performed by striking an arc between a coated-metal electrode and the base metal. Once the arc has been established, the molten metal from the tip of the electrode flows together along with the molten metal from the edges of the base metal to form a sound joint. This process is known as fusion. The coating from the electrode forms a covering over the weld deposit, shielding it from contamination; therefore the process is called shielded metal arc welding. The process requires sufficient electric current to melt both the electrode and a proper amount of base metal. It also requires an appropriate gap between the tip of the electrode and the base metal or the molten weld pool. These requirements are necessary to set the stage for coalescence. The sizes and types of electrodes for shielded metal arc welding define the arc voltage requirements (within the overall range of 16 to 40 V) and the amperage requirements (within the overall range of 20 to 550 A). The main advantages of shielded metal arc welding are that high-quality welds are made rapidly at a low cost.

Top view of mild steel specimens

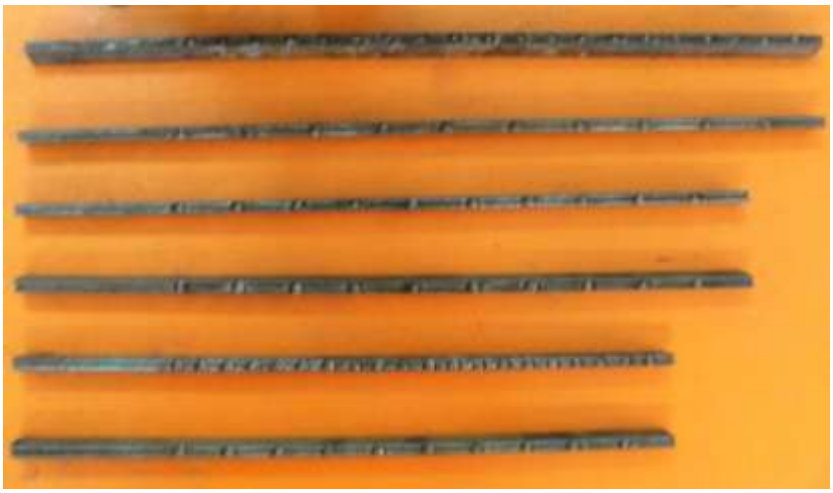

Side view of mild steel specimens

Fig 5.1 Photographs of a few mild steel specimens

Table 5.1 Details of mild steel welded specimens with thickness ratio 1.0

Thickness × Width (mm × mm)	Number of layers	Number of tack welds	length (mm)
(3+3) × 40.25	2	10	430.34
(4+4) × 40.25	2	20	470.22
(6+6) × 40.25	2	30	510.32
(3+3) × 33.00	2	10	320.36
(4+4) × 33.00	2	20	353.20
(6+6) × 33.00	2	30	386.23

Table 5.2 Details of mild steel welded specimens with thickness ratio 1.5

Thickness × Width (mm × mm)	Number of layers	Number of tack welds	length (mm)
(2+3) × 40.25	2	10	430.34
(2.4+3.6) × 40.25	2	20	470.22
(4+6) × 40.25	2	30	510.32
(2+3) × 33.00	2	10	320.36
(2.4+3.6) × 33.00	2	20	353.20
(4+6) × 33.00	2	30	386.23

Table 5.3 Details of mild steel welded specimens with thickness ratio 2.0

Thickness × Width (mm × mm)	Number of layers	Number of tack welds	length (mm)
(2+4) × 40.20	2	10	430.34
(3+6) × 40.20	2	20	470.22
	2	30	510.32
(2+4) × 40.20	2	10	320.36
(3+6) × 40.20	2	20	353.20
	2	30	386.23

5.3 Description of the Experimental Set-up

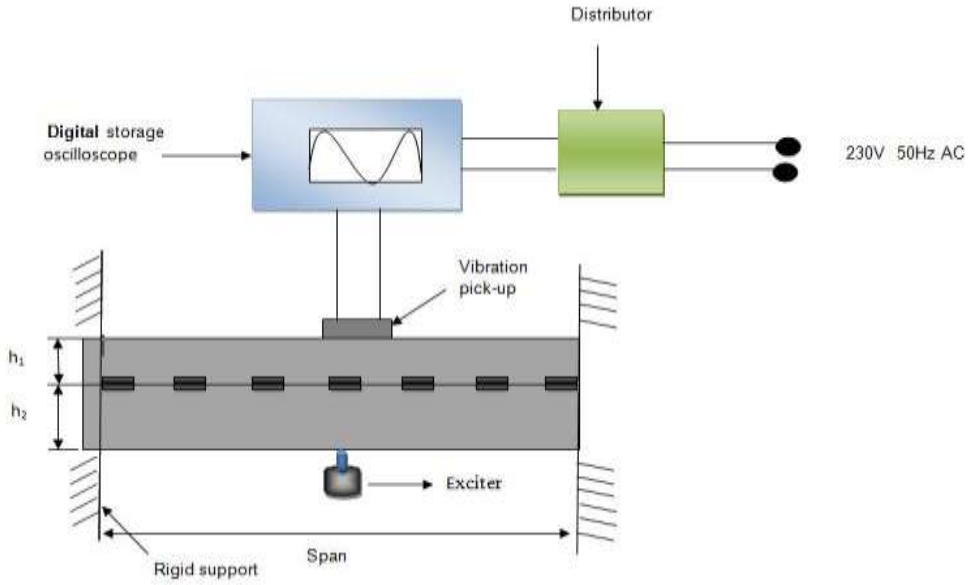

Fig 5.2 Schematic diagram of the experimental set-up

Fig. 5.3 Experimental set-up

The schematic diagram of the experimental set-up with the detailed instrumentation and photographic views are shown in Fig.5.2 and 5.3, respectively.

The test rig includes the following instruments.

1. Power supply unit
2. Digital Storage Oscilloscope
3. Accelerometer/Vibration Pick-Up (Contacting Type Magnetic Probe)
4. Vibration Exciter
5. Dial Gauge

1. Digital storage oscilloscope

A digital storage oscilloscope is a type of electronic instrument which is used for processing and displaying vibration signals. As shown in the above Fig. 5.4 of a digital oscilloscope contains various input connectors, control buttons on the panel to adjust the instrument to get the exact value of signals. The signal to be measured is fed to one of the connectors. It plots a two dimensional graph of the time history curve.

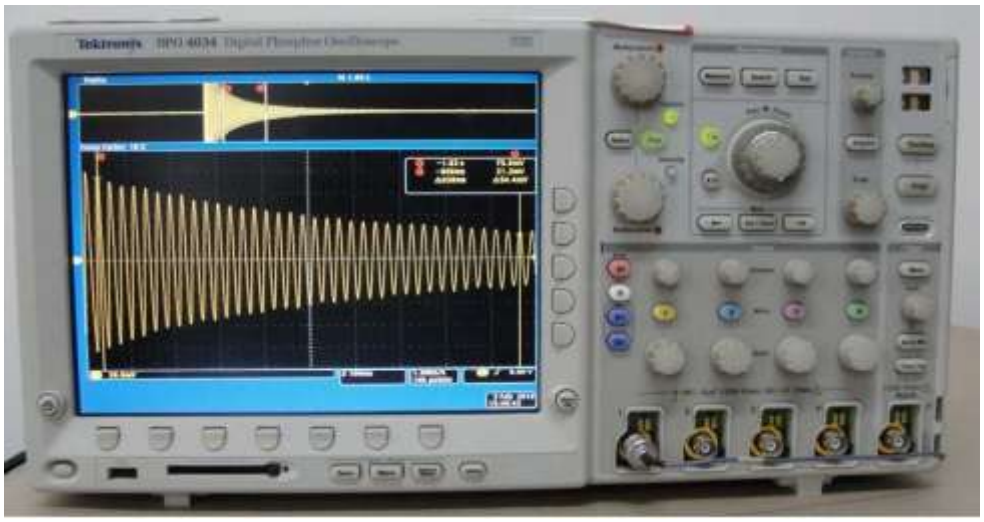

Fig. 5.4 Digital storage oscilloscope

Specifications:

Tektronix 4000 series

DPO 4000 series Oscilloscope

Input Voltage: 100 V to 240 V ± 10%

Input Power Frequency: 47 Hz to 66 Hz (100 V to 240 V)

400 Hz (100 V to 132 V)

Power Consumption: 250 W maximum

Weight: 5 kg (11 lbs), standalone instrument

Clearance: 51 mm (2 in)

Temperature

Operating Temperature: 0 to 50 0C

Humidity

Operating Humidity: High: 40 to 50 0C, 10 to 60% RH

Operating Humidity: Low: 0 to 40 0C, 10 to 90% RH

Altitude

Operating: 3000 m (about 10,000 ft)

Non- operating: 12,192m (40000 ft)

Random Vibration

Operating: 0.31 GRMS, 5 – 500 Hz, 10 minutes per axis, 3 axes (30 minutes total)

Non-operating: 2.46G_{RMS}, 5-500Hz, 10 minutes per axes, 3 axes (30 minutes total)

Pollution Degree: 2, Indoor use only

1. **Exciter**

Fig. 5.5 Vibration Exciter

A vibration exciter (shaker) is an electro-mechanical device which transforms electrical A.C. signals into mechanical vibrations and is used to excite vibrations in bodies or structures for testing purposes. A spring loaded type of exciter is used in this experiment.

Type

V-6-2/050

Make: NAL, Bangalore

2. **Contacting type vibration pick-up**

Fig. 5.6 Accelerometer

The vibration pick-up is a device that transforms the mechanical quantities, such as displacement, velocity or acceleration into electrical quantities, such as voltage or current. These are various types such as contacting and non-contacting type. In the present work contacting type vibration pick-up is used. One end of the accelerometer is a magnetic base which is attached to the vibrating surface and the other end is connected to the first connector port of the storage oscilloscope. The accelerometer used in the experiments is shown as in Fig. 5.6.

Specifications:-

Type: - MV-2000.

- Dynamic frequency range: - 2 c/s to 1000 c/s
- Vibration amplitude: - ±1.5 mm max.
- Coil resistance: - 1000Ω
- Operating temperature: - 10ċ to 40 ċ
- Mounting: - by magnet
- Dimensions: - cylindrical Length:-45 mm Diameter: - 19 mm
- Weight: - 150 grams

3. **Dial gauge**

Fig. 5.7 Dial gauge mounted on a stand with magnetic base

Dial gauge instruments are used for accurate measurement of a small distance. They may also be known as a Dial test indicator (DTI), or as a "clock". They are named so because the measurement results are displayed in a magnified way by means of a dial. Dial indicator may be used to check the variation in tolerance during the inspection process of a machined part, measure the deflection of a beam under dynamic loading conditions, as well as many other situations where a small measurement needs to be indicated. The dial gauge as shown in Fig. 5.7 is shock proof and can measure the amplitude of excitation in the range of 0.01 to 10 mm.

4. **Distributor box**

A distribution box supplies the AC power to the storage oscilloscope at a voltage and frequency of 230V and 50Hz, respectively.

5.4 Testing procedure

In order to find out the damping capacity of jointed beams experimentally and compare it with the theoretical results, an experimental set-up is used to compare the theoretical value with the experimental value. For this some experiments are conducted on the prepared specimens. The various measurement techniques used for the calculation of the value of the Young's modulus of elasticity, static bending stiffness and theoretical logarithmic decrement.

5.4.1 Measurement of young's modulus of elasticity

The Young's modulus of elasticity (E) of the specimen material is found out by conducting static deflection tests. For this purpose, few samples of solid specimen beams are selected from the same stock of mild steel flats. These specimens are mounted on the same experimental set-up rigidly so as to ensure perfect boundary conditions for fixed-fixed beam. Static loads (W) are applied at the mid-span and the corresponding deflections (Δ) are recorded. The Young's modulus for the specimen material is then determined using the expression $E=WL^3/ 192I\Delta$, where L and I are the free length and moment of inertia of the fixed-fixed specimen. The average of some readings is recorded from the tests from which the average value of Young's modulus for different material is evaluated and is found to be 197.6 GN/m^2 for mild steel specimens.

5.4.2 Measurement of static bending stiffness

The stiffness of a welded joint beam is less than the stiffness of a solid beam. That means the stiffness of the beam is used to be decreased due to joints present in the structure. The reduction in the stiffness of the structure is also called stiffness ratio. This can be represented as the ratio of stiffness of jointed beam to that of the solid beam. The value of stiffness ratio is much more important for the actual calculation of logarithmic damping decrement. The same static deflection tests are conducted as in case of Young's modulus are performed to measure the actual stiffness (k) of a jointed specimen using the relation $k=W/\Delta$. However, the stiffness of an identical solid fixed-fixed mild steel beam is theoretically calculated from the expression $k'=192EI/L^3$. The average values of the stiffness ratios for two layered fixed-fixed beams jointed with tack weld has been calculated by using the above two expressions. Further, the stiffness ratio of multi-layered jointed beams has been calculated in the similar manner as in case of two layered ones for thickness ratio 1.0.

5.4.3 Measurement of Damping

Once, the Young's modulus and static bending stiffness of the specimen materials are determined, tests are further conducted on the same set of specimens for evaluating the damping capacity. In the present study, damping has been measured using the logarithmic decrement methods based on time domains.

5.4.3.1 Logarithmic Damping Measurement

The logarithmic decrement technique is the most popular time-response method used for measuring the damping. The logarithmic decrement represents the rate at which the amplitude of a free damped vibration decreases. As the structure is considered to vibrate with small excitation level in the low and moderate frequency range, this method produces fairly good results for lightly damped linear systems. In this method, the structure is set into free vibration with the fundamental mode dominating the response since all the higher modes are damped out quite quickly. The vibration response of the specimen is picked up by the accelerometer and a time history curve showing the decay of amplitude is displayed on the digital storage oscilloscope. This decay can be further used to estimate the damping in jointed specimens using the expression $\delta = \frac{1}{n}\ln\left(\frac{x_0}{x_n}\right)$, where x_0, x_n and n are the recorded values of the amplitudes of the first cycle, last cycle and the number of cycles, respectively.

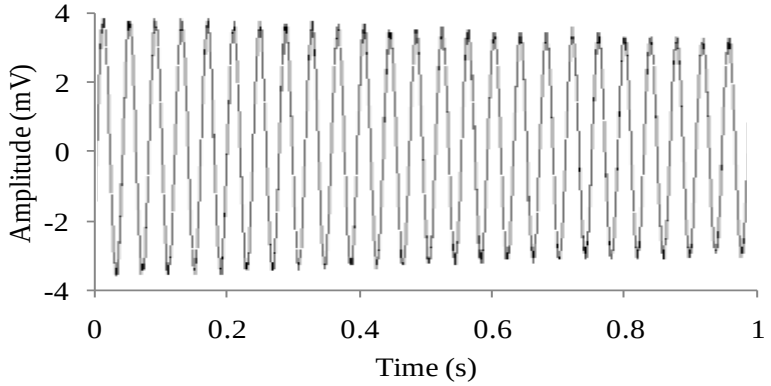

Two layered mild steel specimen (510.65x40.25x6) mm Amplitude of excitation = 0.1 mm Time history curve of welded mild steel specimens under free vibration recorded by the digital storage oscilloscope.

5.5 Experimental Evaluation of "$\alpha.\mu$"

These two parameters are to be measured for the evaluation of the logarithmic decrement correctly. They are inter-dependent with each other and inversely related. Further, they exhibit complex behaviour under dynamic condition making it difficult to assess the exact value of the individual parameters at a particular condition of excitation. In view of the above factors, it is convenient to evaluate the product $\alpha.\mu$ as a single parameter from the experimental results and use it for theoretical calculations for other conditions of the beam. However, their product $\alpha.\mu$ is found to be constant for a particular specimen under a particular condition of vibration irrespective of surface roughness.

The product $\alpha.\mu$ has been determined from the experimental results of logarithmic decrement for two layered welded fixed-fixed beam specimens of mild steel using expression (3.31). Since this product is frequency and amplitude dependent, plots displaying its variation with the above two parameters are shown in Figs. 5.8 to 5.10 for mild steel specimens. These plots are further used to find out the numerical values of the logarithmic decrement for other conditions of the beam using expressions (3.27) and (3.30). It is observed from the above plots that this product increases with an increase in both the natural frequency and amplitude of excitation. In order to validate this, experiments are conducted with a few layered and welded beams made up of mild steel with different thickness ratio and excited at 0.1 mm.

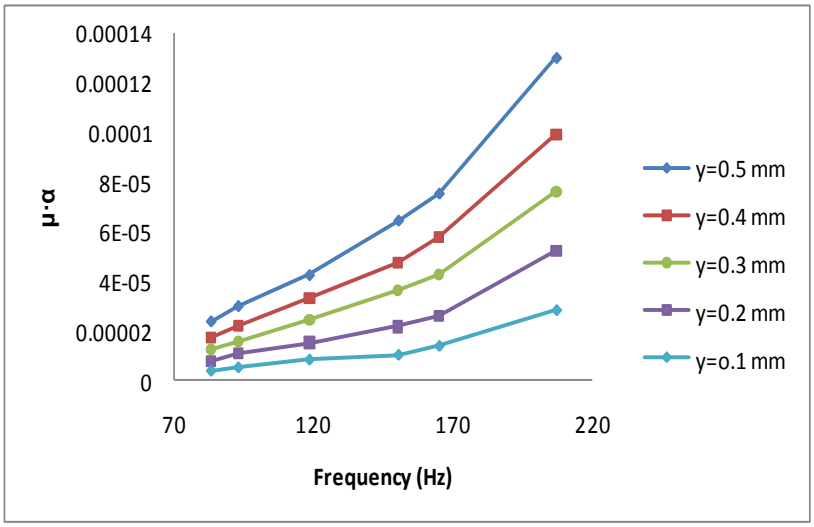

Fig.5.8 Variation of $\alpha.\mu$ with frequency of vibration for mild steel specimens with beam thickness ratio 1.0 at different initial amplitudes of excitation (y)

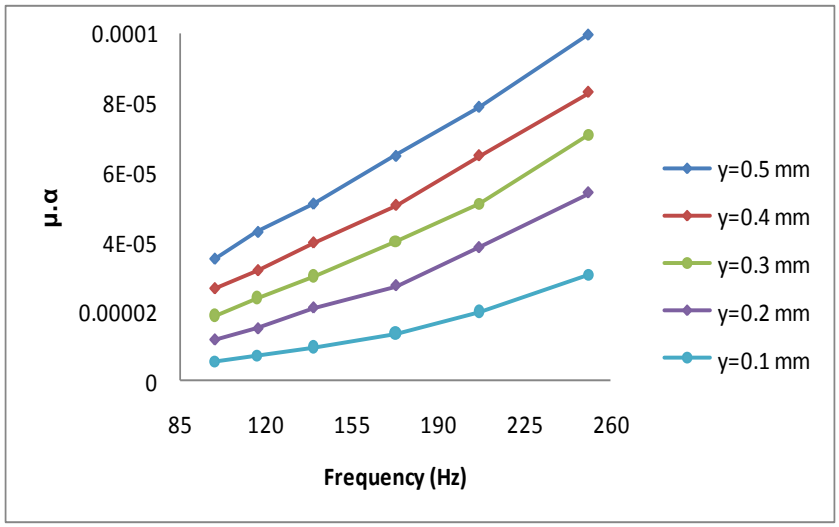

Fig.5.9 Variation of $\alpha.\mu$ with frequency of vibration for mild steel specimens with beam thickness ratio 1.5 at different initial amplitudes of excitation (y)

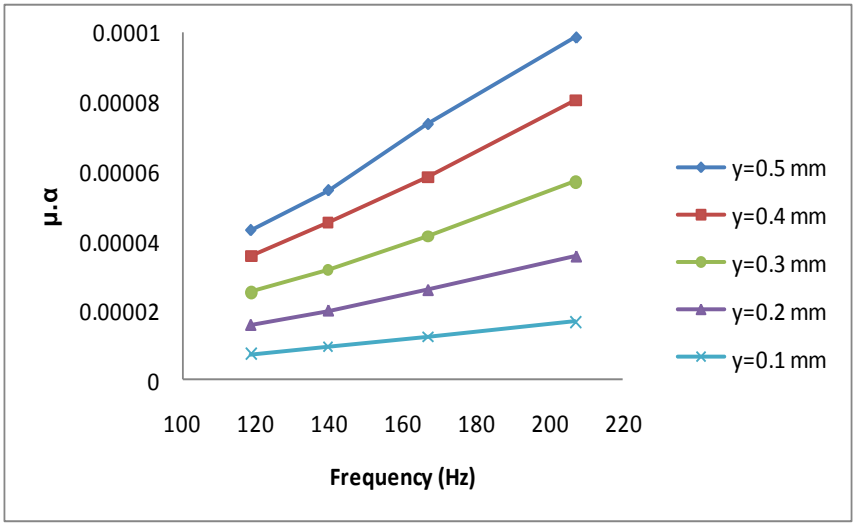

Fig. 5.10 Variation of $\alpha.\mu$ with frequency of vibration for mild steel specimens with beam thickness ratio 2.0 at different initial amplitudes of excitation (y)

CHAPTER 6

RESULTS AND DISCUSSION

6.1 Results

The results are compared and presented in graphical forms. In all these plots, the numerical results obtained either by classical or finite element method is shown by solid lines (——) and the corresponding experimental ones by dashed lines (- - -).

6.1.1 Logarithmic Decrement of Welded Beams Based on Theoretical Analysis Considering Dynamic Slip Ratio

A classical method is used to formulate the expressions (3.27) and (3.31) for evaluating the logarithmic decrement and product $\alpha.\mu$, respectively. The logarithmic decrements of various specimens are found out using expression (3.30) using the product $\alpha.\mu$ determined from Figs. 5.8 to 5.10 at different frequencies and amplitudes of vibration. In this section, the comparison of the results by the classical approach and experiments has been shown in Figs. 6.1 to 6.2 for mild specimens. It is observed from the above results that both the curves are close to each other with maximum variation of 5.05%.

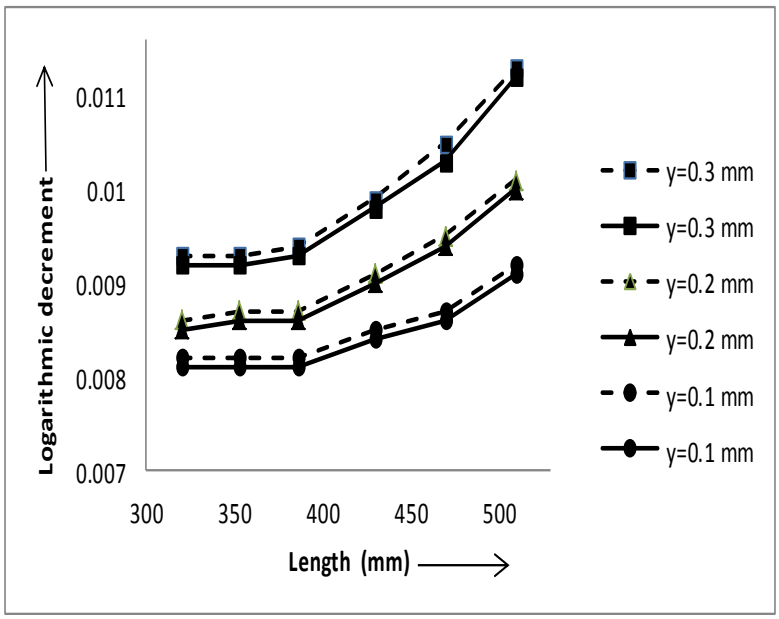

Fig. 6.1 Variation of logarithmic decrement (δ) with length for welded mild steel beams

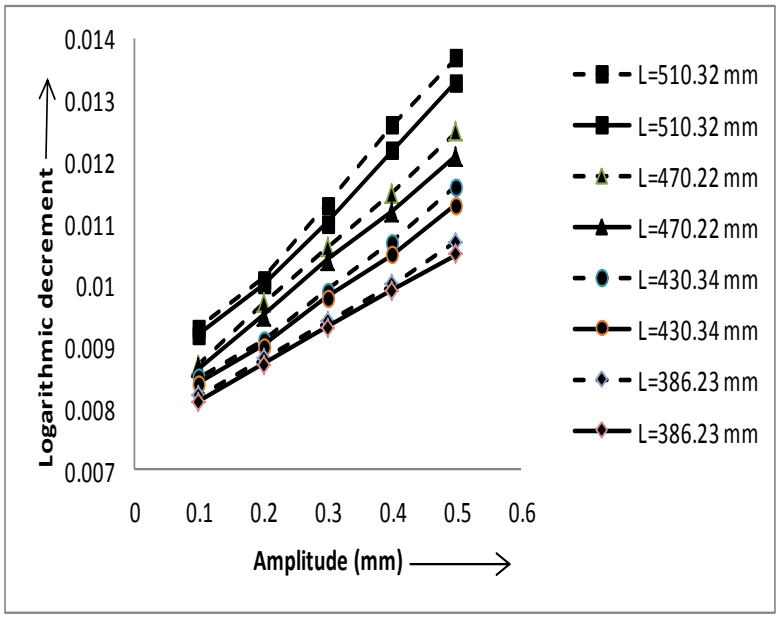

Fig. 6.2 Variation of logarithmic decrement (δ) with amplitude for welded mild steel beams of dimensions in mm

Table 6.1 Effect of influencing parameters on the damping capacity of mild steel beams

Length × thickness × width (mm × mm × mm)	Influencing parameter	Variation of influencing parameter	Variation in damping capacity
470× (3+3) ×40.25 (with 0.4 mm amplitude)	Beam length	Increases from 386.23 to 510.32 mm	Increases by 8.21%
510× (3+3) ×40.25	Amplitude of vibration	Increases from 0.1 to 0.5 mm	Increases by 6.73%

6.2 Discussion

The damping mechanism in welded structures is influenced by the intensity of pressure distribution, micro-slip and kinematic coefficient of friction at the interfaces. The damping in layered and welded structures is dependent on various dimensional parameters such as; length and thickness of the specimen, amplitude of vibration, number of layers and thickness ratio of the welded beam laminates. The following observations have been made from the theoretical and experimental analyses in the process of investigation.

1. The exact nature of the interface pressure profile and its magnitude across a beam layer is necessary for the proper estimation of the damping capacity of welded structures. The welded beams are considered to be in contact with each other because of perfect flatness. Since perfect contact is maintained under both the static and dynamic conditions, the pressure at the interfaces is taken to be uniform. In the present investigation the pressure distribution given by Johnson [25] and Giannakopoulos et al. [26] for flat surfaces in contact with each other has been used for the analysis.

2. The presence of friction at the interfaces due to the welded joints has a strong influence on the system dynamics and largely contributes to the majority of the damping capacity of the system. It is understood that the interface friction comes into play only when the contacting layers tend to move relatively under the action of transverse vibration and serves as a medium for energy dissipation. In the present analysis, the Coulomb's friction law is used to represent the friction at the contacting surfaces.

3. The energy dissipation at the interfaces of jointed structures primarily depends upon the kinematic coefficient of friction (μ) and dynamic slip ratio (α). These two parameters are interdependent with each other and exhibit complicated behaviour under dynamic conditions. In view of the above facts, it is more appropriate to evaluate the product $\alpha.\mu$ as a single parameter from the experimental logarithmic decrement corresponding to welded beam of particular thickness. Since this product is frequency and amplitude dependent, plots have been drawn in Figs. 5.7 to 5.9 for the mild steel specimens. These plots have been further used for the theoretical evaluation of logarithmic decrements of layered and welded beams with respect to other dimensions and conditions of vibration.

4. The joints usually do not form a rigid connection and thus allow a relative motion at the interfaces of the connecting members. As the beam vibrates, it bends in the transverse direction. This beam bending causes the generation of shear stresses at the contact surfaces. The slippage being of extremely small amount is termed as micro-slip and occurs only at the lower level of excitation. This small relative displacement at the interfaces causes energy dissipation due to friction thereby contributing large amount of damping to the system. When the excitation level is increased, the macro-slip is developed due to which the entire jointed interface will slip as a whole. Usually, the macro-slip is avoided as it leads to structural damage of the joints.

5. In the present work, damping capacity of layered and welded structures has been examined for the following variables: length and thickness of the specimen, amplitude of vibration, number of layers and thickness ratio. The dependency of the damping on each of these variables is enumerated from the theoretical and experimental results as discussed below.

   (a) The damping capacity of the welded mild steel structures increases with the increase in length as presented in Table 6.1. The variation of damping capacity with length of welded symmetrical and unsymmetrical mild steel specimens is plotted as shown in Figs. 6.1. From the figures, it is evident that the damping capacity increases with the increase in length. With the increase in length, the interface area is increased resulting in greater dissipation of the energy due to friction.

   (b) The damping capacity of the welded mild steel structures increases with the increase in initial amplitude of excitation as presented in Table 6.1. The variation of damping capacity with initial amplitude of excitation for welded symmetrical and unsymmetrical mild steel specimens are plotted as shown in Figs. 6.2. From the figures, it is evident that the damping capacity increases with the increase in initial amplitude of vibration at the mid-span of the beam model; the amplitude of vibration raises the energy loss due to friction.

CHAPTER 7

CONLUSION AND SCOPE OF FUTURE WORK

7.1 Conclusion

The damping of welded structures in the present investigation has been examined for the following variables: intensity of pressure distribution, dynamic slip ratio, kinematic coefficient of friction at the interfaces, length of the specimen, amplitude of vibration. The effect of all these parameters on the damping capacity of layered and welded structures is enumerated from the theoretical and experimental results as detailed below.

The damping capacity of a layered beam jointed with tack weld increases with:

- increase in the length of beam
- increase in initial amplitude of excitation

7.2 Scope for Further Research

- Timoshenko beam theory can be used for analysis instead of Euler-Bernoulli beam theory.
- The problem can be analysed nonlinearly instead of a linear problem.
- The analysis can be made for layered and jointed beams of dissimilar materials.
- The analysis can be made for layered and jointed plates

REFERENCE

1. Groper, M., June 1985, Microslip and macroslip in bolted joints, ExperimentalMechanics, pp. 171-174
2. Hartwigsen, C.J., Song, Y., Mcfarland, D.M., Bergman, L.A. and Vakakis, A.F.,2004, Experimental study of non-linear effects in a typical shear lap jointconfiguration, Journal of Sound and Vibration, Vol. 277, No. 1-2, pp. 327-351.
3. Pratt, J.D. and Pardoen, G., 2002, Numerical modeling of bolted lap jointbehaviour, Journal of Aerospace Engineering, Vol. 15, No. 1, pp. 20-31.
4. Masuko, M., Ito, Y. and Yoshida, K., 1973, Theoretical analysis for a dampingratio of a jointed cantibeam, Bulletin of JSME, Vol. 16, No. 99, pp. 1421-1432
5. Nishiwaki, N., Masuko, M., Ito, Y. and Okumura, I., 1978, A study on dampingcapacity of a jointed cantilever beam, 1st Report: Experimental results, Bulletinof JSME, Vol. 21, No. 153, pp. 524-531
6. Nishiwaki, N., Masuko, M., Ito, Y. and Okumura, I., 1980, A study on dampingcapacity of a jointed cantilever beam, 2nd Report: Comparison betweentheoretical and experimental values, Bulletin of JSME, Vol. 23, No. 177, pp.469-475
7. Olofsson, U. and Hagman, L., 1997, A model for micro-slip between flatsurfaces based on deformation of ellipsoidal elastic bodies, TribologyInternational, Vol. 30, No. 8, pp. 599-603.
8. Thomson, W.T., 1993, Theory of Vibration with Applications, 2nd Edition,George Allen and Unwin, London.
9. Den Hartog, J.P., 1931, Forced vibrations with combined coulomb and viscousfriction, Transactions of the ASME, Vol. 53, No. 9, pp. 107-115.
10. Goodman, L.E. and Klumpp, J.H., 1956, Analysis of slip damping withreference to turbine-blade vibration, ASME, Journal of Applied Mechanics, Vol.23, pp. 421–429.
11. Motosh, N., 1975, Stress distribution in joints of bolted or riveted connections,ASME, Journal of Engineering for Industry, Vol. 97, No. 1, pp. 157-161.
12. Gould, H.H. and Mikic, B.B., 1972, Areas of contact and pressure distribution inbolted joints, ASME, Journal of Engineering for Industry, Vol. 94, No. 3, pp.864–870.

13. Ziada, H.H. and Abd, A.K., 1980, Load pressure distribution and contact areasin bolted joints, Institute of Engineers (India), Vol. 61, pp. 93–100.
14. Nanda, B.K. and Behera, A.K., 1999, Study of damping in layered and jointedstructures with uniform pressure distribution at the interfaces, Journal of Soundand Vibration, Vol. 226, No. 4, pp.607-624.
15. Minakuchi, Y., Koizumi, T. and Shibuya, T., 1985, Contact pressuremeasurement by means of ultrasonic waves using angle probes, Bulletin ofJSME, Vol. 28, No. 243, pp. 1859-1863.
16. Masuko, M., Ito, Y. and Koizumi, T., 1974, Horizontal stiffness and micro-slipon a bolted joint subjected to repeated tangential static loads, Bulletin of JSME,Vol. 17, No. 113, pp. 1494-1501.
17. Beards, C.F., 1983, The damping of structural vibration by controlled interfaceslip in joints, ASME, Journal of Vibration, Acoustics, Stress and Reliability andin Design, Vol. 105, No. 3, pp. 369–373.
18. Olunloyo, V.O.S., Osheku, C.A. and Damisa, O., 2008, Vibration damping instructures with layered viscoelastic beam-plate, ASME, Journal of Vibration andAcoustics, Vol. 130, No. 6, pp. 061002-(1-26).
19. Damisa, O., Olunloyo, V.O.S., Osheku, C.A. and Oyediran, A.A., 2008,Dynamic analysis of slip damping in clamped layered beams with non-uniformpressure distribution at the interface, Journal of Sound and Vibration, Vol. 309,No. 3-5, pp. 349-374.
20. Gaul, L. and Lenz, J., 1997, Nonlinear dynamics of structures assembled bybolted joints, ActaMechanica, Vol. 125, No. 1-4, pp. 169-181.
21. Sainsbury, M.G. and Zhang, Q.J., 1999, The Galerkin element method applied tothe vibration of damped sandwich beams, Computers and Structures, Vol. 71,No. 3, pp. 239-256.
22. Lee, S.Y., Ko, K.H. and Lee, J.M., 2000, Analysis of dynamic characteristics ofstructural joints using stiffness influence coefficients, KSME InternationalJournal, Vol. 14, No. 12, pp. 1319-1327.
23. Chen, W. and Deng, X., 2005, Structural damping caused by micro-slip alongfrictional interfaces, International Journal of Mechanical Sciences, Vol. 47, No.8, pp. 1191-1211.
24. Oldfield, M., Ouyang, H. and Mottershead, J.E., 2005, Simplified models ofbolted joints under harmonic loading, Computers and Structures, Vol. 84, No. 1-2, pp. 25-33.

25. Giannakopoulos, A.E., Lindley, T.C., Suresh, S. and Chenut, C., 2000, Similarities of stress concentrations in contact at round punches and fatigue at notches: Implications to fretting fatigue crack initiation, Fatigue and Fracture of Engineering Materials and Structures, Vol. 23, No. 7, pp. 561–571
26. Earles, S.W.E., 1966, Theoretical estimation of the frictional energy dissipation in a simple lap joint, IMechE, Part C: Journal of Mechanical Engineering Science, Vol. 8, No. 2, pp. 207–214.
27. Clough, R.W. and Penzien, J., 2003, Dynamics of Structures, 3rd edition, Computers and Structures, Inc., Berkeley, USA.